Generalized entropies in a turbulent dynamo simulation

Axel Brandenburg

Nordita, Blegdamsvej 17, DK-2100 Copenhagen Ø, Denmark

Isaac Klapper

Department of Mathematics, University of California, Los Angeles, California 90024

Jürgen Kurths

Max-Planck-Arbeitsgruppe "Nichtlineare Dynamik," Universität Potsdam, D-14415 Potsdam, Germany

(Received 10 May 1995)

A simulation of hydromagnetic turbulence exhibiting dynamo action is employed to estimate the generalized entropies, H_q, from the distribution of moments of local expansion factors of material line elements. These generalized entropies can be used to characterize the dynamics of turbulence and of nonlinear dynamo action. The value of the metric entropy, H_1, is comparable to the largest Lyapunov exponent describing the divergence of trajectories in phase space, which in turn is somewhat larger than the growth rate of the magnetic energy. The value of the topological entropy, H_0, is similar to the conversion rate of kinetic to magnetic energy, but larger than the growth rate of the dynamo. This is in agreement with results stating that the growth rate of the kinematic dynamo is limited by the topological entropy. The dependence of H_q on q leads to a criterion from which we infer that the degree of intermittency in our particular system is weak.

PACS number(s): 47.27.Eq, 47.52.+j

Metric and topological entropies are important quantities that characterize the degree of chaos in dynamical systems. Topological entropy in particular has relevance for dynamo theory due to its close connection to the stretching of curves of finite extent [1]. Thus magnetic field growth at least at large magnetic Reynolds numbers can be related to the topological entropy [2] when well defined. In a dynamo, kinetic energy is continuously converted into magnetic energy through field line stretching so the magnetic field can grow and can be sustained against Ohmic dissipation.

The generalized entropies H_q characterize the dynamical behavior of the system. They are the counterpart of the generalized dimensions that characterize spatial properties of a snapshot in time [3–5]. Generalized entropies have previously been used in the context of kinematic dynamo theory [6]. The topological entropy H_0 is frequently used to characterize the degree of chaos in maps [7]. Nevertheless topological entropy does not seem to be a widely used tool in turbulence physics. In the present paper we consider data of a three-dimensional simulation of hydromagnetic convection exhibiting dynamo action [8]. The generalized dimensions have previously been estimated [9] for this simulation. Our aim is to gain more detailed information about the dynamical characteristics of this simulation in order to obtain a better understanding of magnetic field amplification and saturation.

In the idealized case without magnetic diffusion, the evolution both of magnetic field lines and of material lines is described by the Cauchy solution [10]

$$B_i(\boldsymbol{\xi},t) = \mathcal{D}_{ij}(\boldsymbol{\xi},t)B_j(\mathbf{x},0), \qquad (1)$$

where $\mathcal{D}_{ij} \equiv \partial \xi_i / \partial x_j$ is the displacement gradient matrix and $\boldsymbol{\xi}(\mathbf{x},t)$ is the position of a particle initially at $\mathbf{x} = \boldsymbol{\xi}(\mathbf{x},0)$. For a short time interval δt we have

$$\mathcal{D}_{ij}(\boldsymbol{\xi},\delta t) = \delta_{ij} + \delta t \frac{\partial u_i}{\partial x_j}(\boldsymbol{\xi},0). \qquad (2)$$

The finite time displacement gradient matrix along individual particle trajectories $\boldsymbol{\xi}(\mathbf{x},t)$ can be obtained iteratively from the matrix of the previous time step by matrix multiplication

$$\mathcal{D}_{ij}(\boldsymbol{\xi},t+\delta t) = \left[\delta_{ik} + \delta t \frac{\partial u_i}{\partial x_k}(\boldsymbol{\xi},t) \right] \mathcal{D}_{kj}(\boldsymbol{\xi},t), \qquad (3)$$

where δt is now the time step used in this simulation. We compute $\mathcal{D}$ for a large number of trajectories and extract the three eigenvalues σ_j, where $|\sigma_1| > |\sigma_2| > |\sigma_3|$. The expansion factors are the moduli of σ_j, which can be computed directly from the eigenvalues of the matrix $\mathcal{D}^T \mathcal{D}$. It turns out that the expansion rates from $|\sigma_2|$ are small compared to those of $|\sigma_1|$ (see below). Therefore we estimate the generalized entropies from the moments of $\epsilon \equiv |\sigma_1|$ alone, using [11]

$$H_q(\tau) = \frac{1}{1-q} \frac{1}{\tau} \ln \langle \epsilon^{1-q} \rangle, \qquad (4)$$

where $\tau = t - t_0$ is the time since the initialization of the trajectories on a uniform mesh at $t = t_0$. The angular brackets denote averages, which are here taken to be over all trajectories. The degree of convergence may be judged from Fig. 1, where we plot the dependence of $H_q(\tau)$ and τ. In that plot we also include the corresponding results for the other two eigenvalues. In principle we are interested in the limit $\tau \to \infty$, but in practice we are forced to use the last time available from the data. Thus we set $H_q = H_q(\tau_{\max})$ expecting however that this will somewhat overestimate the actual value. We are of course unable to address questions of infinite time convergence here.
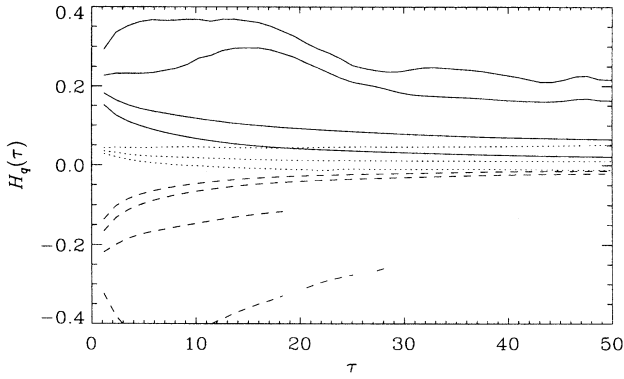
FIG. 1. Dependence of $H_q(\tau)$ (solid lines) versus τ, for four different values of q ($q = -1, 0, 1,$ and 2). The dotted and dashed lines give the corresponding results for the other two eigenvalues. For each eigenvalue the uppermost curve is for $q = -1$. (When σ_3 is too small, no results are plotted.)

In the case $q \to 1$ we expand $\langle \epsilon^{1-q} \rangle = 1 + (1-q)\langle \ln\epsilon \rangle$ and then expand the logarithm in Eq. (4) to obtain $H_1 = (1/\tau)\langle \ln\epsilon \rangle$. This expression resembles the ordinary Lyapunov exponent except for the fact that for Lyapunov exponents, expansion in phase space is considered. The expansion in phase space was investigated in an earlier paper [12] using data from the same simulation. Here, instead, the expansion in real space is the relevant quantity for understanding magnetic field amplification. It will turn out, however, that the two are not very different. Also we note that $H_0 = (1/\tau)\ln\langle \epsilon \rangle$ is similar to topological entropy, differing principally in the fact that we did not include the possible contribution from expanding surface elements. The same is also true for the metric entropy. In other words, to estimate the topological and metric entropies we should have included the expansion rates from $|\sigma_2|$ at those points where $\ln|\sigma_2| > 0$. However, as can be seen from Fig. 1, this would only lead to a minor modification because the second expansion rate is small (the sum of all three expansion rates is close to zero due to weak compressibility).

At an early stage of our investigations we integrated the particle trajectories using a frozen velocity field, that is, a velocity field taken from a snapshot in time of the dynamo simulation in the saturation phase. The generalized entropies for the frozen velocity field are surprisingly similar to those for the evolving field, which was obtained by restarting the simulation from the snapshot mentioned above. For cross-reference with other work analyzing the same data [8,9,12,13], we mention that the time of the snapshot is 779 time units, where time is measured in units of free fall times. One turnover time is about 20 time units. The resolution is $63 \times 63 \times 63$ mesh points, and this is also the number of trajectories used to estimate H_q. In our simulation the deep layers beneath the convection zone proper are included. In those layers the system is stable to convection and motion only results from fluid elements that shoot over into the convectively stable layer. In the analysis presented below we restrict ourselves to the convection zone proper to avoid the large number of trajectories with almost no expansion of line elements, which would significantly distort the results.

TABLE I. Comparison of H_0 and H_1 with the largest Lyapunov exponent λ_1, and the growth rate of the dynamo λ_{dyn}. Results are given both for the saturated phase and the growth phase, as well as for a frozen velocity field ($\tau = 27$). Finite time effects may be judged by comparison with a somewhat longer run (growth$_*$: $\tau = 50$; frozen$_*$: $\tau = 46$). In the last two columns the magnetic field production rate $\lambda^{(B)}$ and the normalized variance μ (see below) are also given.

Rate	H_0	H_1	λ_1	λ_{dyn}	$\lambda^{(B)}$	μ
saturated	0.13	0.10	0.08	0	0.135	0.036
growth	0.15	0.12		0.05	0.134	0.044
frozen	0.14	0.11				0.050
growth$_*$	0.13	0.09		0.05	0.134	0.047
frozen$_*$	0.13	0.09				0.049

In order to investigate the effects of magnetic field saturation on the dynamics we also present results where we restarted with a fresh seed magnetic field. This case is referred to as the growth phase of the dynamo. Unless stated otherwise, the results presented below refer to the growth phase obtained in this way. We should note that during the growth phase of the dynamo the magnetic field is still weak and does not significantly affect the velocity field. In that sense we are still in a (statistically) stationary regime as far as the expansion rates of line elements are concerned.

In Table I we compare the H_0 and H_1 with other typical inverse time scales in the problem (all in units of inverse free fall times). Evidently, H_0 is the largest of the various rates given in the table. Furthermore, H_1 is comparable with the largest Lyapunov exponent that was obtained earlier [12] by computing the rate of divergence between two slightly perturbed trajectories in phase space. The magnetic field instantaneous production rate in the direction of stretching [13], $\lambda^{(B)} = \langle B_i^{(str)} B_j^{(str)} s_{ij} \rangle / \langle \mathbf{B}^2 \rangle$, is comparable to H_0. Here, s_{ij} is the rate of strain matrix and $\mathbf{B}^{str}$ is the magnetic field vector in the direction of the largest eigenvector of s_{ij}, i.e., in the direction of stretching.

We remark again that H_0 is closely related to the stretching rate of curves of finite extent which is in turn closely related to the topological entropy [if the intermediate expansion rate $(1/\tau)\ln|\sigma_2| \sim 0$ as expected, then the two are approximately equal]. Even for the saturated case, the value of H_0 is larger than the dynamo growth rate λ_{dyn} during the earlier growth phase prior to saturation. Table I also shows that between the saturated and the growth phases of the dynamo the difference in H_0 is small. This suggests that exponential line stretching is still present during the saturated stage and is not quenched to any significant degree. In fact, the main dynamo saturation mechanism is apparently Joule dissipation adjusting itself to balance the magnetic field growth, i.e., the work done against the Lorentz force [8]. This is also supported by the fact that the production term in the direction of stretching, $\lambda^{(B)}$, is clearly larger than the growth rate and in fact is comparable to H_0.

We should point about that the apparent similarity in the values of H_1 and the phase space Lyapunov exponent λ_1 may be coincidental. The L_1 norm of the difference between two trajectories in phase space, which was used to compute

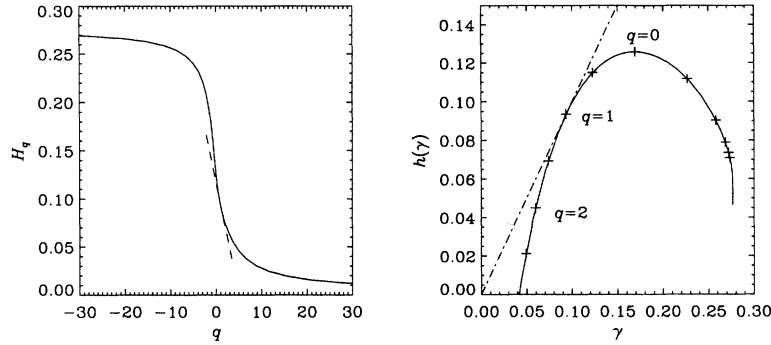AXEL BRANDENBURG, ISAAC KLAPPER, AND JÜRGEN KURTHS

FIG. 2. Generalized entropies H_q and their spectrum $h(\gamma)$ for the growth phase ($\tau = 50$). Some values of q (equally spaced between -2.5 to 2.5) are indicated in the plot of $h(\gamma)$. The dashed curve in the H_q plot is the tangent at $q = 1$.

λ_1, could be considered as being similar to the average expansion rate $\langle \epsilon \rangle$ of line elements. In that sense, the definition of λ_1 appears to be more similar to $H_0 = (1/\tau)\ln\langle \epsilon \rangle$ than to $H_1 = (1/\tau)\langle \ln\epsilon \rangle$. Note, however, that the expansion rates in phase space include not only field line stretching but also expansion rates of other quantities, including fluid density, temperature, and velocity. Furthermore, when measuring the expansion rates in phase space, the effects of dissipation are automatically included, whereas the expansion of line elements (computed from the Cauchy solution) excludes dissipation effects. Therefore we expect H_0 to be an upper bound to λ_1, as is indeed the case here.

We now turn our attention to the entropy spectrum $h(\gamma)$. Analogously to the $f(\alpha)$ singularity spectrum for fractal dimensions [14], we compute $h(\gamma)$ via a Legendre transformation,

$$h(\gamma) = q\gamma - \Psi_q, \quad \gamma = \frac{d\Psi_q}{dq}, \quad (5)$$

where $\Psi_q = (q-1)H_q$. [We follow here the notation of Yoshida and So [5].] In Fig. 2 we plot H_q and $h(\gamma)$. For $q = 1$, $h(\gamma)$ has the tangent $h(\gamma) = \gamma$, and for $q = 0$, $h(\gamma)$ is maximal. It is possible to interpret $h(\gamma)$ as the topological entropy of the set of trajectories associated with a given value of γ [5,15]. The fractal dimension of this set of points is equal to $h(\gamma)/\gamma$ [15].

In the analogous case of fractal dimensions one can alternatively compute the $f(\alpha)$ singularity spectrum directly using the histogram of probabilities [16]. This method can also be used to estimate the entropy function from the histogram of local expansion rates [4]. In the present case we can com-

pute the probability density function $p(\gamma)$, where $\gamma = (1/\tau)\ln\epsilon$ is now defined locally along each trajectory. In order to compute $h(\gamma)$ directly we have to consider the relationship between $p(\gamma)$ and H_q. In general, the average over different trajectories in Eq. (4) can be replaced by an integral weighted with $p(\gamma)$, so

$$H_q = \frac{1}{1-q}\frac{1}{\tau}\ln \int e^{\tau(1-q)\gamma} p(\gamma)d\gamma. \quad (6)$$

The Legendre transformation used to obtain Eq. (5) assumes that $p(\gamma)$ is of the form

$$p(\gamma) = \phi(\tau)e^{-\tau[\gamma - h(\gamma)]}, \quad (7)$$

where $\phi(\tau)$ is a normalization factor such that $\int p(\gamma)d\gamma = 1$. Since $\gamma - h(\gamma)$ is never positive, $p(\gamma)$ has a sharp maximum in the limit of large values of τ. This allows us to use the saddle point method for large τ to obtain

$$H_q = \frac{1}{q-1}\min_{\gamma}[q\gamma - h(\gamma)], \quad (8)$$

showing that with Eq. (7), $h(\gamma)$ is indeed the Legendre transformation of $\Psi_q \equiv (q-1)H_q$. We also see from Eq. (7) that $h(\gamma)$ can be estimated from $p(\gamma)$ via

$$h(\gamma) = \gamma + \frac{1}{\tau}\ln[p(\gamma)/\phi(\tau)], \quad (9)$$

where $\phi = \max(p)$. In Fig. 3 we compare $h(\gamma)$ as obtained via the two different methods. It can be seen that there is good agreement between the two methods. Also consistent
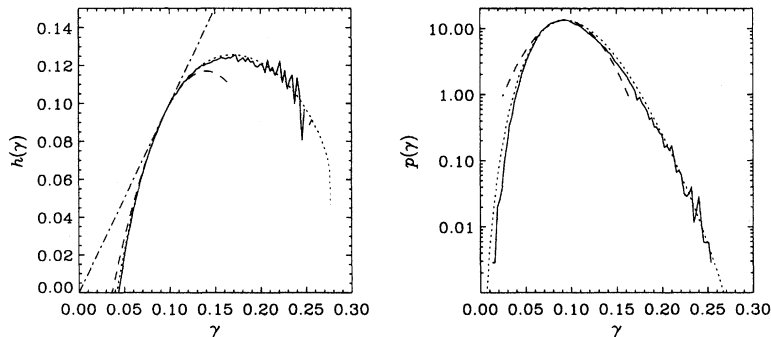

FIG. 3. Left panel: Comparison of $h(\gamma)$ as obtained via H_q (dotted line) with $h(\gamma)$ as obtained directly from $p(\gamma)$ (solid line). the dashed line refers to the result for a Gaussian distribution of γ. The diagonal $h = \gamma$ (dashed-dotted line) is shown for comparison. Right panel: Comparison of the actual histogram $p(\gamma)$ (solid line) with the histogram implied by Eq. (7) (dotted line), and with the Gaussian distribution of γ, see Eq. (7).

with earlier results [17], we note that the indirect method via the moments is more stable than the histogram method for obtaining the $f(\alpha)$ spectrum. However, for negative values of q the data are more noisy. In the right-hand panel of Fig. 3 we compare the actual histogram with Eq. (7). Again, the agreement is good.

These results are for the growth phase of the dynamo with $\tau_{max} = 50$. For the saturated phase we only have $\tau_{max} = 27$. This is rather short, and results in poor convergence of the $h(\gamma)$ curve, especially for negative values of q. We also should point out that if we had included the deep layers beneath the convection zone proper in our analysis, our histogram would have had a second hump near $\gamma = 0$ due to the extended regions in the flow where the dynamics is very mild. The analysis presented above (using the saddle point method) would not be valid for such peculiar distribution functions. In that case there should be poor agreement between the histogram and indirect methods for computing $h(\gamma)$.

The two numbers H_0 and H_1 can be used to characterize the dynamics of the system. We find that in our case the value of H_1 is typically 30% smaller than H_0. On the other hand, very different values of H_0 and H_1 would indicate that the dynamics of the system are highly nonuniform, i.e., intermittent. This can be formulated more quantitatively using the slope of H_q near $q = 1$; see the dashed line in Fig. 2. If H_q was strictly linear, then

$$H_q = \lambda - \tfrac{1}{2}\mu(q-1) \qquad (10)$$

(the $\tfrac{1}{2}$ factor is chosen to be consistent with Crisanti *et al.* [18]); this would correspond to a purely Gaussian distribution $p(\gamma)$ with

$$p(\gamma) = e^{-(\gamma-\lambda)^2/(2\sigma^2)}/\sqrt{2\pi\sigma^2}, \qquad (11)$$

where $\lambda = \langle \gamma \rangle$ and $\mu = \tau\sigma^2$ with $\sigma^2 = \langle \gamma^2 \rangle - \lambda^2$. Of course, this is a reasonable fit only in the narrow interval $-0.5 < q < 2.5$, as is shown by the dashed curves in Fig. 3. In that figure we have also plotted the $h(\gamma)$ curve implied by Eq. (9), i.e.,

$$h(\gamma) = \gamma - (\gamma-\lambda)^2/(2\mu). \qquad (12)$$

Using Eq. (10) in Eq. (4) it can be shown that $\lambda = H_1$ is equal to the average value $\langle \gamma \rangle$, and that $\tfrac{1}{2}\mu = dH_q/dq|_{q=1}$ is equal to τ times the variance $\langle (\gamma-\lambda)^2 \rangle$. In Table I the values of μ and $\lambda = H_1$ are given for various cases. The fact that the ratio μ/λ is less than unity indicates [18] that our system is only weakly intermittent.

In conclusion, we have presented a feasible method of estimating generalized entropies using the displacement gradient matrix. The generalized entropies are used to characterize the nature of dynamo action from a given flow field, both during as well as before the saturation phase. The $h(\gamma)$ curve can be estimated both directly from the histogram of local expansion rates as well as indirectly via the spectrum of generalized entropies. We suggest that estimating generalized entropies could be a fruitful diagnostic tool in turbulence research.

---

[1] Y. Yomdin, Israel J. Math. **57**, 285 (1987); S. E. Newhouse, Ergod. Theor. Dyn. Syst. **8**, 283 (1988).

[2] J. Finn and E. Ott, Phys. Fluids **31**, 2992 (1988); M. M. Vishik (private communication); I. Klapper and L. S. Young, Comm. Math. Phys. (to be published).

[3] P. Grassberger and I. Procaccia, Physica **13D**, 34 (1984); R. Badii and A. Politi, Phys. Rev. A **35**, 1288 (1987); H. Fujisaka, R. Hagihara, and M. Inoue, *ibid.* **38**, 3680 (1988).

[4] P. Grassberger, R. Badii, and A. Politi, J. Stat. Phys. **51**, 135 (1988).

[5] T. Yoshida and B. C. So, Prog. Theor. Phys. **79**, 1 (1988).

[6] M. Falcioni, G. Paladin, and A. Vulpiani, Europhys. Lett. **10**, 201 (1989); S. A. Molchanov, A. A. Ruzmaikin, and D. D. Sokoloff, Geophys. Astrophys. Fluid Dyn. **30**, 242 (1984).

[7] For example, N. J. Balmforth, E. A. Spiegel, and C. Tresser, Phys. Rev. Lett. **72**, 80 (1994).

[8] Å. Nordlund, A. Brandenburg, R. L. Jennings, M. Rieutord, J. Ruokolainen, R. F. Stein, and I. Tuominen, Astrophys. J. **392**, 647 (1992).

[9] A. Brandenburg, I. Procaccia, D. Segel, and A. Vincent, Phys. Rev. A **46**, 4819 (1992).

[10] H. K. Moffatt, *Magnetic Field Generation in Electrically Conducting Fluids* (Cambridge University Press, Cambridge, 1978); E. N. Parker, *Cosmical Magnetic Fields* (Clarendon, Oxford, 1979).

[11] E. Ott, *Chaos in Dynamical System* (Cambridge University Press, Cambridge, 1994).

[12] J. Kurths and A. Brandenburg, Phys. Rev. A **44**, R3427 (1991).

[13] A. Brandenburg, Chaos, Solitons & Fractals **5**, 225 (1995).

[14] T. C. Halsey, M. H., Jensen, L. P. Kadanoff, I. Procaccia, and B. I. Shraiman, Phys. Rev. A **33**, 1141 (1986).

[15] T. Bohr and D. Rand, Physica **25D**, 387 (1987).

[16] A. Chhabra and R. V. Jensen, Phys. Rev. Lett. **62**, 1327 (1989).

[17] A. Crisanti, G. Paladin, and A. Vulpiani, *Products of Random Matrices in Statistical Physics* (Springer-Verlag, Berlin, 1993).

[18] A. Crisanti, M. H. Jensen, G. Paladin, and A. Vulpiani, Phys. Rev. Lett. **70**, 166 (1993).